JOURNAL OF BACTERIOLOGY, Sept. 1990, p. 5200–5210
0021-9193/90/095200-11$02.00/0

Vol. 172, No. 9

Identification of a VirB10 Protein Aggregate in the Inner Membrane of *Agrobacterium tumefaciens*

JOHN E. WARD, JR.,[1]†* ELIZABETH M. DALE,[1] EUGENE W. NESTER,[2] AND ANDREW N. BINNS[1]

Plant Science Institute, Department of Biology, University of Pennsylvania, Philadelphia, Pennsylvania 19104-6018,[1] and Department of Microbiology, School of Medicine, University of Washington, Seattle, Washington 98195[2]

Received 21 March 1990/Accepted 15 June 1990

Products of the *virB* operon are proposed components of a membrane-associated T-DNA transport apparatus in *Agrobacterium tumefaciens*. Here we identified the *virB10* gene product and raised specific antiserum to the protein. While the *virB10* reading frame contains two potential ATG translation start sites located 32 codons apart, we found that only the downstream ATG was required for efficient VirB10 synthesis. Cellular localization studies and analysis of translational fusions with the *Escherichia coli* alkaline phosphatase gene (*phoA*) indicated that VirB10 was anchored in the inner membrane and contained a periplasmic domain. This work also demonstrated the utility of alkaline phosphatase as a reporter for secreted proteins in *A. tumefaciens*. Several high-molecular-weight forms of VirB10 were observed after treatment of *A. tumefaciens* whole cells or inner membranes with protein cross-linking agents, suggesting that VirB10 exists as a native oligomer or forms an aggregate with other membrane proteins. These results provide the first biochemical evidence that a VirB protein complex is membrane associated in *A. tumefaciens*.

The soil bacterium *Agrobacterium tumefaciens* initiates crown gall tumor formation in plants by transferring a segment of DNA (the T-DNA) from the Ti plasmid of the bacterium into the plant cell nucleus (for reviews see references 3, 43, and 44). This remarkable process is mediated, in part, by the virulence (*vir*) gene products that are encoded by at least seven operons in octopine-type Ti plasmids, designated *virA*, *-B*, *-C*, *-D*, *-E*, *-G*, and *-H* (15, 27). The results from numerous studies concerning the structure and function of the *vir* gene products have revealed similarities between the processes of T-DNA transfer and bacterial conjugation. Thus, it has been proposed that the *vir* genes are functionally analogous to the *tra* genes of conjugative plasmids (28, 44, 45). This model is supported by the finding that the *mob* and *oriT* functions of a small mobilizable plasmid (pRSF1010) can generate a DNA molecule capable of passage to plant cells through the activities of the *vir* gene transfer machinery (4). Although some of the early *vir*-mediated events in T-DNA processing are becoming understood, the mechanism by which the T-DNA molecule is transported across both the bacterial and plant cell membranes and walls remains unknown. In the best-characterized bacterial conjugal transfer system, that of the *Escherichia coli* F plasmid, a number of F plasmid *tra* gene products are believed to form a membrane-spanning DNA transfer pore after juxtaposition of the donor and recipient cells (13, 38). Therefore, it is possible that an analogous membrane-associated T-DNA transfer complex is encoded by the *vir* genes of *A. tumefaciens*.

Products of the Ti plasmid *virB* operon are candidates to form such a T-DNA transfer complex for several reasons. First, polar transposon insertions within the *virB* operon completely abolish virulence, suggesting that at least some of the VirB proteins are required for T-DNA transfer (27). Second, nucleotide sequence analysis of the ~9.5-kilobase-pair (kbp) *virB* operon from three Ti plasmids revealed that of the 11 predicted *virB* proteins, most are likely to be membrane associated (16a, 30, 36, 37), and three VirB proteins have been localized to the bacterial envelope (9). In more recent work, the VirB11 protein was found to associate extrinsically with the *A. tumefaciens* inner membrane, and biochemical studies demonstrated that VirB11 is an ATPase that can be autophosphorylated (6). The predicted *virB11* gene product also displays amino acid sequence similarity with *comG*ORF1, a protein required for the uptake and passage of DNA through the cell wall of competent *Bacillus subtilis* cells (1). Like VirB11, *comG*ORF1 contains a consensus nucleotide-binding domain and is part of an operon encoding a number of potential membrane-associated proteins. These findings suggest that three different bacterial processes involving DNA transport across a membrane barrier, i.e., T-DNA transfer, conjugal exchange of plasmids, and bacterial transformation, all utilize a membrane protein transport apparatus. Furthermore, the finding that VirB11 binds ATP and is an ATPase suggests that T-DNA transport is regulated by VirB11 phosphorylation, or by the VirB11-mediated phosphorylation of other VirB proteins that compose a membrane transfer channel. Further characterization and precise cellular localization of the VirB proteins thus appears essential to understand the mechanism of T-DNA transfer. Here we report a biochemical analysis of the *virB10* gene product that was predicted by a recent revision of the original pTiA6 *virB* operon nucleotide sequence (36, 37). Our results indicate that VirB10 has a transmembrane topology and is a component of an inner membrane protein complex in *A. tumefaciens*.

MATERIALS AND METHODS

Reagents and enzymes. Acetosyringone (AS), isopropyl-β-D-thiogalactopyranoside (IPTG), 5-bromo-4-chloro-3-indoyl-phosphate (X-P), *p*-nitrophenyl phosphate, *p*-Nitro Blue Tetrazolium, *N*-ethylmaleimide, phenylmethylsulfonyl fluoride, 3β-indoleacrylic acid, lysozyme, kanamycin, chloramphenicol, and carbenicillin were purchased from Sigma Chemical Co. (St. Louis, Mo.). Tween 20, trizma base,

* Corresponding author.
† Present address: Department of Biological Sciences, Southern Methodist University, Dallas, TX 75275-0376.

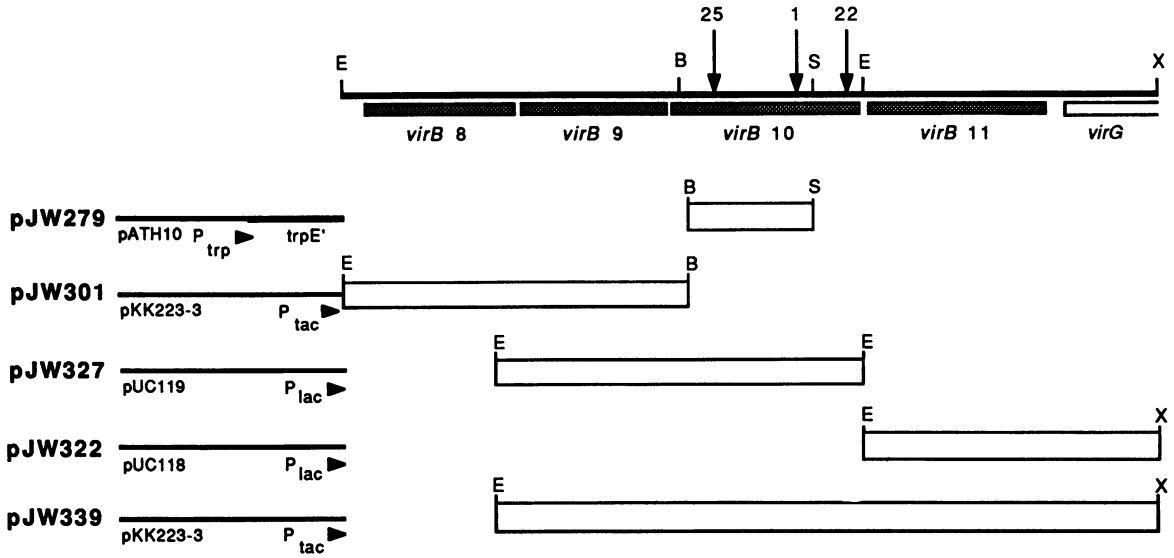

FIG. 1. Plasmid vectors for the analysis of genes from the 3′ end of the pTiA6 *virB* operon. Vector sequences are represented by lines, and the directions of transcription from the expression vector promoters are indicated by the arrowheads. Locations of the predicted *virB* genes (36, 37) are indicated by the shaded rectangles. The restriction endonuclease sites used to subclone the *virB*-containing DNA fragments are shown on the top line and abbreviated as follows: B, *Bam*HI; E, *Eco*RI, S, *Sal*I, X, *Xho*I. In the construction of pJW327 and pJW339, an *Eco*RI site was introduced within the 3′ end of *virB8* as described in Materials and Methods. The arrows locate Tn*phoA* (20) insertions in *virB10* as determined by DNA sequence analysis.

alkaline phosphatase-conjugated goat anti-rabbit and goat anti-mouse immunoglobulin Gs, and nitrocellulose paper were obtained from Bio-Rad Laboratories (Richmond, Calif.). Bis(sulfosuccinimidyl) suberate (BS^3) and dimethyl 3,3′-dithiobispropionimidate (DTBP) were purchased from Pierce Chemical Co. (Rockford, Ill.). Restriction endonucleases and T4 DNA ligase were purchased from either Bethesda Research Laboratories, Inc. (Gaithersburg, Md.) or International Biotechnologies, Inc. (New Haven, Conn.). S1 nuclease (from *Aspergillus oryzae*) and *E. coli* exonuclease III were from Bethesda Research Laboratories. ^{35}S-labeled dATP, ^{35}S-labeled methionine, and the in vitro *E. coli* transcription-translation kit were obtained from Amersham Corp. (Arlington Heights, Ill.). Sequence analysis was done with the PC-Gene program from Intelligenetics, Inc. (Mountain View, Calif.).

Strains and growth conditions. *A. tumefaciens* A348 is strain A136 containing pTiA6NC (10). A derivative of this strain also contained pToK9 (14), a plasmid that enhances *vir* gene expression. The bacteriophage vector M13mp18 (40) and *E. coli* MV1190 and CJ236 were obtained from Bio-Rad Laboratories. Strain JW100 (36) was used to propagate and maintain plasmid vectors, and the *phoA*-deleted strain CC159 was obtained from Colin Manoil (University of Washington, Seattle). All growth media, bacterial and phage growth conditions, and procedures for *vir* gene induction were as described previously (7), except that *vir* inductions were performed for 14 h in the presence of 200 μM AS.

Plasmid constructions. All procedures for plasmid DNA isolation and manipulation were as described by Maniatis et al. (19). Plasmid pJW200 contains the 3.9-kbp *Sal*I 12 fragment from pTiA6 cloned into pUC119 (31) such that transcription of the *virB* genes was opposite that of the *lac* promoter on the vector. A deletion derivative of pJW200 was constructed by digestion with *Xba*I and *Kpn*I, treatment with exonuclease III and S1 nuclease, and then blunt-end ligation with T4 DNA ligase. DNA sequence analysis (Sequenase kit; U.S. Biochemical Corp., Cleveland, Ohio) of the resulting plasmid, pΔ25-200, showed that the *Eco*RI site of the vector was located 230 base pairs from the predicted start codon of the *virB9* gene. Plasmid pJW325 was then made by subcloning a 1.8-kbp *Sal*I-*Xho*I fragment containing the 3′ end of *virB10*, all of *virB11*, and the 5′ end of *virG* into the *Sal*I site of pΔ25-200. Next, plasmid pJW329 was constructed by cloning the 1.53-kbp *Eco*RI-*Pst*I fragment from pJW325 into the expression vector pKK223-3 (Pharmacia LKB Biotechnology Inc). The *virB9*, *virB10*, and *virB11* genes were then placed under *tac* promoter control by inserting the 2.1-kbp *Pst*I fragment from pJW325 into the *Pst*I site of pJW329 to give pJW339 (Fig. 1). The *virB9* and *virB10* genes were placed under *lac* promoter control in plasmid pJW327 by cloning the 2.2-kbp *Eco*RI fragment from pJW325 into pUC119. The construction of plasmids pJW322 (6), pJW301 (36), and pJW279 (36) has been described previously.

Isolation of Tn*phoA* translational fusions. The methods used for λ::Tn*phoA* infection (20), identification of Tn*phoA* insertion plasmids, and alkaline phosphatase assays were as described previously (39). The *virB10*::Tn*phoA* fusion junctions were determined by DNA sequence analysis with an oligonucleotide primer complementary to the end of Tn*phoA*. Expression of the expected VirB10-PhoA fusion proteins was then confirmed by immunostaining analysis with rabbit anti-*E. coli* alkaline phosphatase antiserum (obtained from Steve Lory, University of Washington, Seattle). The *virB10*::*phoA* fusion genes from p327-25 and p327-22 (Fig. 1) were cloned out as *Hin*dIII fragments and inserted under *lac* promoter control in pRK404 (8) to give the plasmids p404-25 and p404-22, respectively. A348 cells containing these *virB10*::*phoA* plasmids were grown in MG/L medium (7) containing 3 μg of tetracycline per ml at 28°C to an optical density at 600 nm of 0.5 and then assayed for alkaline phosphatase activity.

Oligonucleotide mutagenesis. All mutagenesis procedures were done as outlined in the MUTA-GENE M13 mutagenesis kit (Bio-Rad Laboratories). Oligodeoxynucleotides were

synthesized on a Biosearch 8600 DNA synthesizer and purified with columns from Applied Biosystems. The 2.2-kbp *Eco*RI fragment from pJW327 was cloned into M13mp18 such that *virB9* and *virB10* transcription was directed by the *lac* promoter. Single-stranded DNA containing uracil was then isolated from *E. coli* CJ236 and used as the template for mutagenesis reactions. The potential ATG initiation codons of *virB10a* and *virB10b* (see text) were changed to CTG by using the oligonucleotides 5′-CCAGATACAGAGTACTG-3′ and 5′-ATCGTTATTCAGCCCTTTGC-3′, respectively, to prime the in vitro synthesis of the complementary strand. An oligonucleotide primer, 5′-GTCGGAGACCAGGGATC-3′, was then used to confirm the changes by DNA sequence analysis. The 2.2-kbp *Eco*RI fragment was then cloned into pUC119, placing the altered genes behind the *lac* promoter on plasmid pJW327-16 (*virB10a*) and pJW327-15 (*virB10b*). To create an in-frame deletion between *virB10* residues Lys-22 and Lys-55, we used an oligodeoxynucleotide, 5′-TGCG TTGTCATTCACGTCGGAGACCAGGGA-3′, containing bases complementary to the 15 bases on either side of the deletion endpoints, to prime complementary strand synthesis. The presence of the deletion was confirmed by DNA sequencing with a primer, 5′-GCACCTCAATCGGACG-3′, complementary to the template strand from 61 to 76 bases upstream of the fusion junction. The 2.1-kbp *Eco*RI fragment containing the *virB9* and *virB10*Δ22-55 genes was then subcloned into pUC119 with the *virB* genes under *lac* promoter control to give plasmid pJW327Δ22-55. The *virB10* coding region downstream of the *Pst*I site at base pair 8471 (codon 167) (36, 37) in pJW327Δ22-55 was then replaced with a 2.6-kbp *Pst*I fragment from p339-1 containing the entire *phoA* gene and *virB10* gene sequences between the *Pst*I site and the Tn*phoA* insertion site. The resulting plasmid, p327-1Δ22-55, contained the *virB10*::*phoA* fusion gene present in p339-1 as well as the Δ22-55 deletion.

Protein analysis, immunoblotting, and cell fractionation. Protein concentrations were determined with the BCA protein assay reagent (Pierce), using bovine serum albumin (Sigma) as a standard. In vitro synthesis, [^{35}S]methionine labeling of plasmid-encoded proteins, and autoradiography were done as described previously (36). For one-dimensional sodium dodecyl sulfate-polyacrylamide gel electrophoresis (SDS-PAGE), proteins were analyzed by using 0.75-mm 7.0 or 10.0% gels and stained with Coomassie brilliant blue. For quantitation of radioactivity, dried gels were scanned with a phosphoimager (Molecular Dynamics Corp.). The TrpE-VirB10 fusion protein expressed by pJW279 was gel purified (12) from *E. coli* cell lysates and used to raise antiserum in mice (25). Immunoblotting and immunostaining reactions were performed as described previously (7). Apparent molecular weights were estimated by plotting migration distance versus log of the molecular weight, using protein molecular weight markers and prestained markers purchased from Bethesda Research Laboratories. For fractionation of *A. tumefaciens*, AS-induced cells from a 500-ml culture were pelleted and washed three times in 50 mM sodium phosphate (pH 7.6) (PO_4 buffer), suspended in 5.5 ml of PO_4 buffer containing 20% (wt/vol) sucrose, 0.2 mM dithiothreitol, and 0.2 mg each of DNase I and RNase A (Sigma) per ml, and then broken by three passages through a French press at 14,000 lb/in^2. Lysozyme was added to a final concentration of 0.4 mg/ml, and the lysate was incubated on ice for 30 min. Then 5 ml of PO_4 buffer was added, and cell debris was removed by two centrifugations at 20,000 × *g* for 15 min each. The resulting cleared lysate was made 0.2 M with KCl, and the membranes were then pelleted at 150,000 × *g* for 1 h at 4°C in an SW55 Ti rotor. The total membrane pellet was suspended in 1 ml of ice-cold PO_4 buffer by sonication for three 20-s intervals with an extrafine microtip probe at a power setting of 4 (Heat Systems-Ultrasonics, Inc., Farmingdale, N.Y.). The volume was brought up to 5.5 ml with PO_4 buffer, and the membranes were repelleted at 150,000 × *g* for 1 h. Membranes were suspended in 1 ml of 20% sucrose (wt/vol)–3 mM EDTA–0.2 mM dithiothreitol by sonication, and inner and outer membranes were separated by isopycnic sucrose gradient centrifugation (17). Methods for isolation of the periplasmic protein fraction were as described previously (7). The efficiency of fractionation was assessed by measuring the cytoplasmic enzyme marker malate dehydrogenase and the inner membrane marker NADH oxidase. Over 90% of the total malate dehydrogenase activity was routinely present in the soluble protein fraction, while at least 95% of the total NADH oxidase activity was found in the inner membrane fraction.

Protein cross-linking procedures. For cross-linking of whole cells, a 25-ml culture of AS-induced A348 cells containing plasmid pToK9 was pelleted at 10,000 × *g* for 10 min, washed three times in 10 ml of 50 mM PO_4 buffer, and then resuspended in 2.5 ml of PO_4 buffer. A 10 mM stock solution of the homofunctional, noncleavable cross-linking reagent BS^3 (29) was prepared in PO_4 buffer and added at a final concentration of 200 μM to 200 μl of cells in a 1.5-ml microcentrifuge tube. All reaction mixtures were incubated at room temperature for 30 min. Cross-linking reactions were quenched by the addition of 200 μl of 20 mM *N*-ethylmaleimide in 50 mM Tris hydrochloride (pH 7.5) and incubated for 5 min at room temperature. The cells were pelleted in the microcentrifuge, washed once in 200 μl of 50 mM Tris hydrochloride containing 1 mM phenylmethylsulfonyl fluoride and dissolved in 200 μl of SDS sample buffer (0.062 M Tris hydrochloride [pH 6.8], 2% SDS [wt/wt], 10% glycerol, 2% 2-mercaptoethanol [vol/vol], 0.1% bromphenol blue [wt/vol]). All samples were heated at 95°C for 5 min before analysis by SDS-PAGE with 7.0% gels. Inner membrane fractions, which were isolated in approximately 40% sucrose (wt/vol)–3 mM EDTA (pH 8.0)–0.2 mM dithiothreitol, were either dialyzed before use against PO_4 buffer at 4°C or diluted threefold in PO_4 buffer and used directly in cross-linking reactions. There appeared to be no difference in the yield of cross-linked products with either treatment. The membrane protein samples were analyzed by cross-linking with either BS^3 or DTBP (35), a homofunctional reagent which contains an internal disulfide bond that can be cleaved by reduction with 2-mercaptoethanol. Typical reaction mixtures contained 40 μl of membrane protein (between 15 and 17 μg of total protein) containing a final concentration of either 50 or 200 μM BS^3 or 5 mM DTBP. After 30 min of incubation at room temperature, 40 μl of 50 mM Tris hydrochloride (pH 7.5) containing 20 mM *N*-ethylmaleimide was added for 5 min. The BS^3-cross-linked samples were then diluted with 80 μl of SDS sample buffer containing 2% 2-mercaptoethanol and heated at 95°C for 5 min. The DTBP-cross-linked samples were diluted with 80 μl of SDS sample buffer without 2-mercaptoethanol and heated at 70°C for 5 min. For two-dimensional SDS-PAGE, cross-linked proteins (17 μg) were separated in the first dimension through a 1.5-mm 2.5% stacking gel containing 0.125 M Tris hydrochloride (pH 6.8) and 0.4% SDS with a 7% running gel containing 0.125 M Tris hydrochloride (pH 8.0) and 0.4% SDS at 30 mA. A gel slice (5 mm) containing the proteins was cut away and incubated at room temperature for 45 min in 5 ml of 0.125 M Tris hydrochloride (pH 6.8)–0.4% SDS–10%

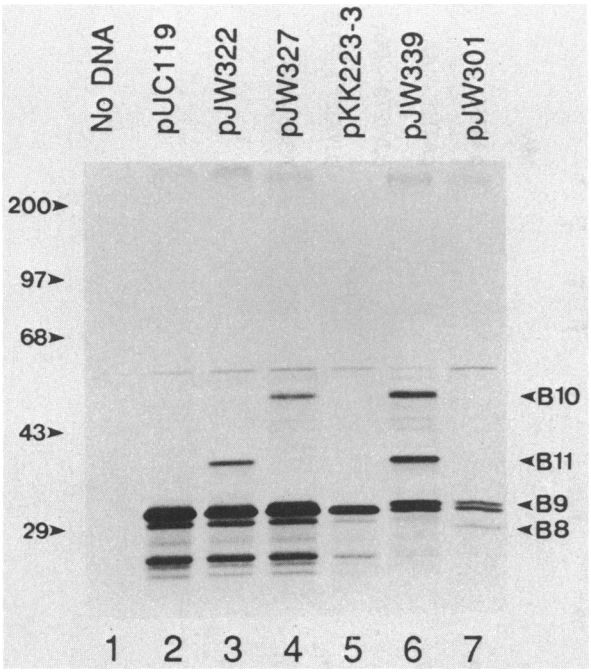

FIG. 2. Identification of VirB proteins. Autoradiograph of proteins expressed from *virB* expression vectors using a coupled in vitro transcription-translation system. [^{35}S]methionine-labeled proteins were separated by SDS-PAGE through a 10% gel followed by autoradiography. The plasmid order is pUC119 (lane 2), pJW322 (lane 3), pJW327 (lane 4), pKK223-3 (lane 5), pJW339 (lane 6), and pJW301 (lane 7). A control lacking plasmid DNA is shown in lane 1. The positions of the potential VirB proteins are indicated. Molecular mass standards (in kilodaltons) include myosin (H chain) (200), phosphorylase *b* (97.4), bovine serum albumin (68), ovalbumin (43), and carbonic anhydrase (29).

(vol/vol) 2-mercaptoethanol. The gel slice was then placed lengthwise onto a 1.5-mm gel containing a 2.5% stacking gel and a 9% running gel for separation in the second dimension.

RESULTS

Identification of *virB10* gene product. A recent revision of the pTiA6 *virB* nucleotide sequence altered the original *virB10* gene reading frame (36, 37), and the structure of the *virB* operon at the 3′ end predicted by the revised sequence is shown in Fig. 1. To confirm the expression of the predicted proteins, we constructed several plasmids, each of which contained a different *virB* DNA restriction fragment cloned such that the *virB* genes were expressed by either the *lac* or *tac* promoter on the vector (Fig. 1). The *virB* plasmid-encoded gene products were then visualized by using an *E. coli* in vitro coupled transcription-translation system. Plasmid pJW327 contained the *virB9* and *virB10* genes placed under *lac* promoter control and encoded two polypeptides with apparent molecular masses (*M*a) of 48 and 32 kilodaltons (kDa), respectively (Fig. 2, lane 4), that were not expressed by the pUC119 vector (lane 2). When the *virB9*, *virB10*, and *virB11* genes were placed under *tac* promoter control in plasmid pJW339, three new proteins of *M*a 48, 38, and 32 kDa, respectively, were detected (compare lane 5 with lane 6). Plasmid pJW301, which had the *virB8* and *virB9* genes placed behind the *tac* promoter, encoded two new proteins of *M*a 32 and 28 kDa, respectively (compare lane 5 and lane 7). These data suggested that the 48-kDa protein could be the *virB10* gene product, which from the revised pTiA6 *virB* nucleotide sequence (37) has a predicted molecular mass (*M*s) of 40,666 Da (but see below). Likewise, the 28- and 32-kDa polypeptides might correspond to the *virB8* (*M*s of 25,382 Da) and *virB9* (*M*s of 32,172 Da) gene products, respectively (37). Finally, the 38-kDa protein represented the previously identified VirB11 protein (6), which was also encoded by pJW339 (Fig. 2, lane 6) and by pJW322, a plasmid containing only the *virB11* gene under *lac* promoter control (lane 3).

VirB10-specific antiserum was used to confirm the identification of the 48-kDa *virB10* gene product. Plasmid pJW279 contains the *trp* promoter and *trpE* gene joined near its carboxyl end in frame to the *virB10* coding sequence between the *Bam*HI site at bp 8018 and the *Sal*I site at base pair 8800 of the revised pTiA6 nucleotide sequence (36, 37). An *M*a 70-kDa fusion polypeptide was encoded by pJW279 that contained almost all the TrpE peptide and 262 amino acids of VirB10 (Fig. 3a, lane 4). This fusion protein was isolated by preparative SDS-PAGE and used to raise antiserum in mice. Immunostaining analysis of proteins expressed from pJW279 after Trp induction in *E. coli* showed that this antiserum reacted strongly with the 70-kDa TrpE-VirB10 fusion protein and with breakdown products of this protein (Fig. 3b, lane 4). The antiserum was found to react only weakly against the 37-kDa TrpE protein (Fig. 3b, lane 3), suggesting that it recognized primarily VirB10 antigenic determinants. A 70-kDa protein that copurified with the fusion protein was also detected weakly in *E. coli* (Fig. 3b, lanes 2 and 3), In *E. coli* cells expressing both the *virB9* and *virB10* genes on plasmid pJW327, the antiserum recognized the 48-kDa VirB10 protein identified in vitro as well as two minor peptides of about 39 and 36 kDa (Fig. 3b, lane 5). However, in extracts of *A. tumefaciens* A348 induced for *vir* gene expression, only the 48- and 39-kDa proteins were detected (Fig. 3b, lane 6). The synthesis of both proteins in *A. tumefaciens* was found to depend on the presence of the Ti plasmid and *vir* gene induction. In addition, we found that *virB* mutant strains containing Tn*3* transposon insertions in either the *virB10* gene or upstream *vir* genes did not express either the 48- or 39-kDa protein, indicating that both were *virB10* gene products (37a).

Mutagenesis of *virB10* translation initiation codon. The predicted *virB10* gene reading frame contains two potential ATG translation initiation codons located 32 codons apart in the same reading frame (Fig. 4a). The corresponding genes, *virB10a* and *virB10b*, would encode predicted proteins of 44,364 and 40,666 Da, respectively (30, 37). To determine the gene from which the 48-kDa VirB10 protein was derived, the predicted ATG start codons were changed to CTG by oligonucleotide-directed mutagenesis. Replacement of an internal ATG codon in the *virB10* gene by CTG, resulting in incorporation of Leu instead of Met, would not be expected to interfere with protein elongation. However, replacement of the initiation codon with CTG would be expected to decrease significantly the level of VirB10 protein synthesis, since CTG is utilized inefficiently as a translation initiation codon in *E. coli* (5). Plasmids containing the wild-type (pJW327), altered *virB10a* (pJW327-16), and altered *virB10b* (pJW327-15) genes under *lac* promoter control were then used as templates in the *E. coli* in vitro protein transcription-translation system. Figure 4b shows an autoradiograph of [^{35}S]methionine-labeled proteins synthesized in vitro and separated by SDS-PAGE. The level of radioactivity present in each 48-kDa VirB10 protein band was determined and normalized to the amount of radioactivity incorporated into

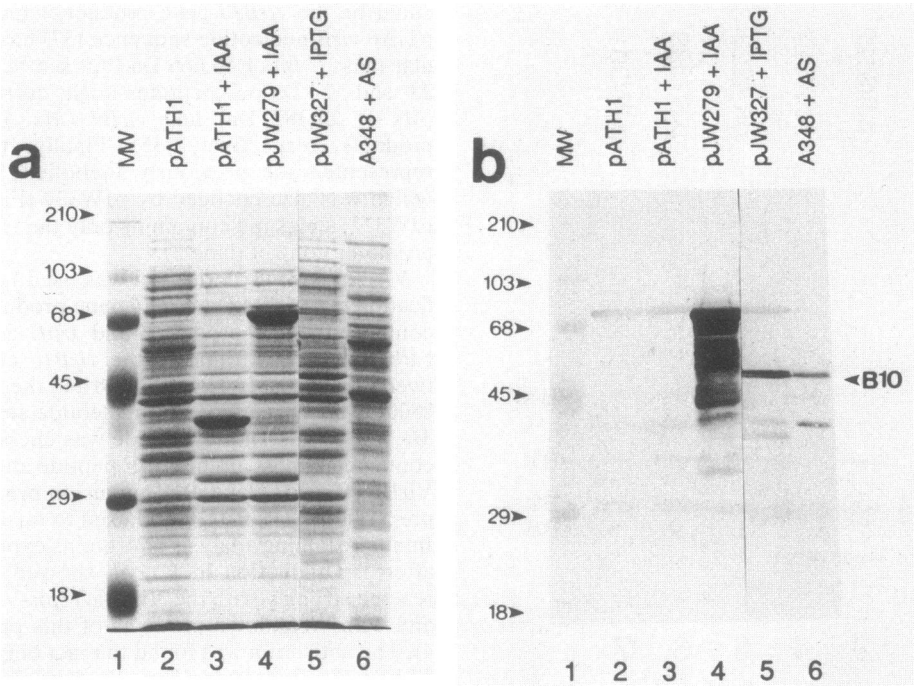

FIG. 3. Immunological identification of the VirB10 protein. (a) Coomassie brilliant blue-stained SDS-10% polyacrylamide gel representing total proteins from *E. coli* JW100 cells containing the following plasmids: pATH1 uninduced (lane 2), pATH1 induced with 3β-indoleacrylic acid (lane 3), pJW279 induced (lane 4), pJW327 induced with IPTG (lane 5). Lane 6 shows proteins present in *A. tumefaciens* A348 cells induced for *vir* gene expression with AS. The prestained protein size standards used (Bethesda Research Laboratories) were calculated to have molecular masses (in kilodaltons) as indicated. (b) Corresponding immunoblot developed with anti-VirB10 antiserum.

the β-lactamase band and an additional common background band. The results indicated that changing the predicted *virB10a* start codon to CTG had no effect on the amount of radioactivity incorporated into VirB10 (Fig. 4b, lanes 3 and 4). However, mutation of the *virB10b* start codon decreased the amount of radioactivity incorporated into the VirB10 protein by 74% compared with pJW327 (Fig. 4b, lanes 3 and 5) and by 78% compared with plasmid pJW327-16 (lanes 4 and 5). The observed decrease in [^{35}S]methionine incorporation into VirB10 with pJW327-15 as a template was much greater than that expected from the loss of one methionine codon in the gene, since the predicted VirB10b protein contains a total of seven methionine residues (30, 36, 37). Furthermore, immunostaining analysis of proteins from IPTG-induced *E. coli* cells revealed a similar decrease in the level of VirB10 synthesis directed by pJW327-15 but no decrease with pJW327-16. From these results, we concluded that the 48-kDa VirB10 protein was the product of *virB10b*, subsequently referred to here as the *virB10* gene.

Cellular localization of VirB10 protein. Computer analysis (PC-Gene) identified a potential membrane-spanning domain located near the amino-terminal end of the predicted VirB10 protein. To determine whether VirB10 was in fact membrane associated, we fractionated cells of strain A348 induced for *vir* gene expression into cytoplasmic, periplasmic, and inner and outer membrane components. The separation profiles of the inner and outer membrane fractions are shown in Fig. 5a, and the protein profiles of the various fractions visualized by SDS-PAGE and Coomassie brilliant blue staining are shown in Fig. 5b. When these fractions were assayed by immunostaining with anti-VirB10 antiserum, the majority of both the 48- and 39-kDa VirB10 proteins were found in the inner membrane fraction (Fig. 5c, lane 5). Neither protein was detected in the free periplasmic protein fraction (Fig. 5c, lane 10).

Isolation and characterization of *virB10*::*phoA* fusions. To investigate the membrane topology of VirB10, we used the vector λ::Tn*phoA* (20) to generate translational fusions with the *E. coli phoA* gene. The *phoA* gene product is active only upon export from the cytoplasm, and the utility of alkaline phosphatase fusions in analyzing membrane protein structure has been described in detail elsewhere (21, 22). Two different Tn*phoA* insertions in pJW327 and one in pJW339 were isolated which gave a PhoA$^+$ phenotype in *E. coli* CC159. The exact fusion junction in these plasmids was determined by nucleotide sequence analysis, and expression of the expected VirB10-PhoA fusion proteins was confirmed by immunostaining analysis with anti-PhoA and anti-VirB10 antiserum. All three VirB10-PhoA fusion proteins displayed high levels of alkaline phosphatase activity, indicating that the PhoA moiety was transported to the periplasm (Table 1).

The *virB10*::*phoA* fusion genes from p327-25 and p327-22 were subcloned under *lac* promoter control into the broad-host-range vector pRK404 (8) to determine whether these fusion proteins displayed a similar activity in *A. tumefaciens*. Cells of *A. tumefaciens* A348 harboring these plasmids grew as dark blue colonies on MG/L plates containing X-P but as very pale blue colonies when containing pRK404 alone. Immunostaining analysis revealed that both VirB10-PhoA fusion proteins were constitutively expressed in *A. tumefaciens*, and both produced significant amounts of alkaline phosphatase activity (Table 1). Cellular fractionation experiments revealed that most of the alkaline phosphatase activity was localized to the inner membrane of *A. tumefaciens* (data not presented). No difference in alkaline phosphatase activity was observed in A348 cells containing the

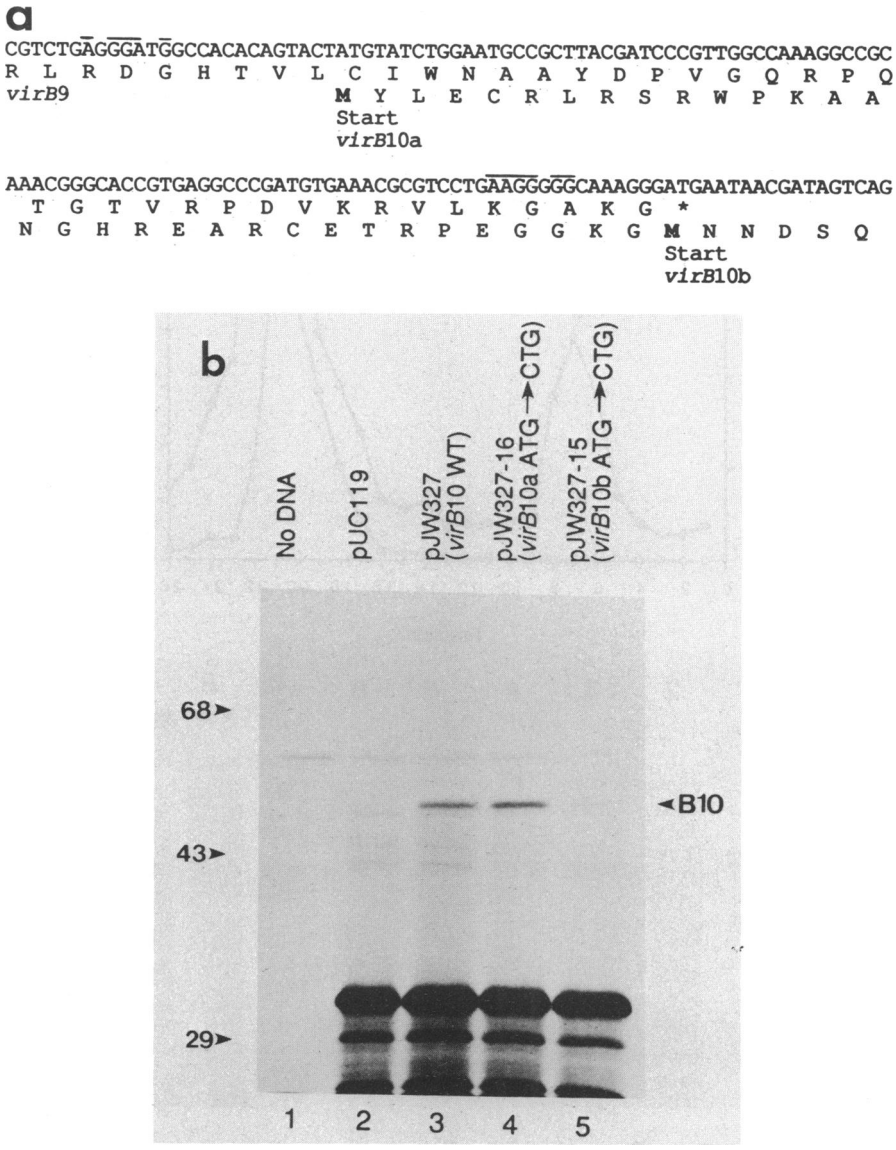

FIG. 4. (a) Nucleotide sequence and predicted amino acid sequences at the junction of the pTiA6 *virB9* and *virB10* genes (37). The start points of the predicted *virB10a* and *virB10b* reading frames are indicated by boldface type, and potential ribosome-binding sites are indicated by the overlined residues. The ATG initiation codons of these *virB10* genes present on plasmid pJW327 were changed to CTG by oligonucleotide-directed mutagenesis as described in Materials and Methods. (b) Autoradiograph showing the effect of *virB10a* and *virB10b* initiation codon mutagenesis on the in vitro synthesis of VirB10. Plasmid DNA (3 μg) was used as a template to synthesize [^{35}S]methionine-labeled proteins in vitro, and an equivalent amount of each reaction mixture was analyzed by SDS-PAGE with a 10% gel. Lane 1, No DNA control; lane 2, pUC119; lane 3, pJW327; lane 4, pJW327-16; lane 5, pJW327-15. The locations of molecular mass standards (in kilodaltons) are indicated on the left.

virB10::*phoA* fusion plasmids after AS induction, indicating that export of the fusion proteins did not depend on *vir* gene functions (unpublished data). These data suggested that much of the VirB10 protein downstream of the predicted transmembrane region between residues 33 and 51 (Fig. 6a) was localized to the periplasm in *E. coli* and *A. tumefaciens*. In addition, this work demonstrated that the alkaline phosphatase protein, which has been used as a reporter for exported proteins in a number of gram-negative organisms (22), can be used to examine protein topology in *A. tumefaciens* as well.

To determine whether the hydrophobic core and flanking charged residues located between residues Lys-22 and Lys-55 (Fig. 6a) were required for VirB10 membrane assembly, we used oligonucleotide-directed mutagenesis to construct an in-frame deletion of this region. When the *virB10*Δ22-55 gene was placed under *lac* promoter control on plasmid pJW327Δ22-55, the expected *M*a 45-kDa protein was expressed after induction with IPTG (Fig. 6b, lane 3). The Δ22-55 deletion was then introduced into the *virB10*::*phoA* fusion gene from p339-1 by restriction fragment replacement to give plasmid pJW327-1Δ22-55. This plasmid directed the synthesis of an *M*a 76-kDa fusion protein (Fig. 6b, lane 4) which displayed a very low level of alkaline phosphatase activity in *E. coli* CC159 (Table 1), indicating that the PhoA moiety was no longer exported to the periplasm. To allow for replication in *Agrobacterium* species, pJW327-1Δ22-55 was joined to the broad-host-range

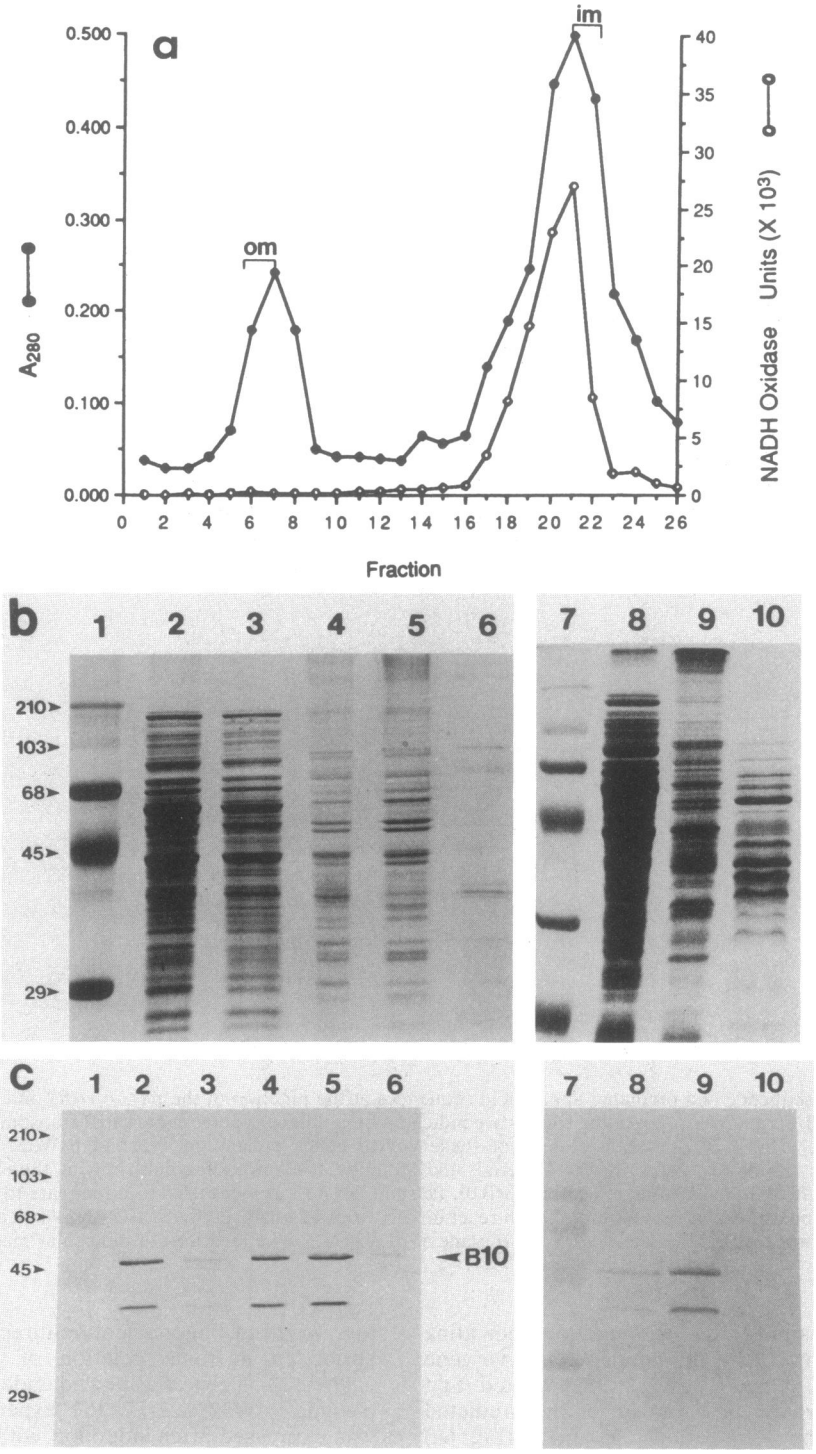

FIG. 5. Localization of the VirB10 protein in *A. tumefaciens* A348. Cells were induced for *vir* gene expression with AS (200 μM) for 14 h and then fractionated as described previously (7, 17). (a) Membrane separation profile, indicating the A_{280} (●) and NADH oxidase (○) values of the fractions obtained after isopycnic sucrose density gradient centrifugation. om, Outer membrane; im, inner membrane. Proteins from the various fractions were separated by SDS-PAGE with duplicate 10% gels and then examined by either Coomassie brilliant blue staining (b) or transfer to nitrocellulose and immunostaining with anti-VirB10 antiserum (c). The sample order in panels b and c is as follows: lanes 1 and 7, molecular mass markers (in kilodaltons); lane 2, total cellular protein; lane 3, soluble protein; lanes 4 and 9, total membrane protein; lane 5, inner membrane protein; lane 6, outer membrane protein; lane 8, cytoplasmic protein; and lane 10, periplasmic protein.

TABLE 1. Characterization of *virB10*::*phoA* gene fusions in *E. coli* CC159 and *A. tumefaciens* A348

virB10::Tn*phoA* insertion plasmid in the following host:		Fusion junction (codon)[a]	Observed fusion protein (kDa)[b]	Alkaline phosphatase activity (U)[c] in:	
E. coli CC159	*A. tumefaciens* A348			*E. coli* CC159	*A. tumefaciens* A348
pUC119	pRK404	None	None	5	4
p327-25	p404-25	82	55	145	285
p339-1	ND[d]	206	79	188	ND
p327-22	p404-22	331	97	146	222
p327-1Δ22-55	pJW401	206Δ22-55	76	7	9

[a] Position of the Tn*phoA* insertion in relation to the predicted translation start point of the *virB10b* gene as determined by nucleotide sequence analysis.
[b] VirB10-PhoA fusion protein molecular mass was estimated by SDS-PAGE and immunostaining with anti-PhoA antiserum.
[c] Cells of *E. coli* CC159 containing either pUC119 or p327-1 were grown to the mid-log phase in LB medium containing 100 μg of carbenicillin per ml and then grown in the presence of 1 mM IPTG for 2 h before determination of alkaline phosphatase activity as described previously (20). Strains containing all other plasmids were first grown in medium containing carbenicillin and kanamycin at 100 μg/ml each and then induced for 2 h with 1 mM IPTG. Plasmid-containing *A. tumefaciens* A348 cultures were grown to the mid-log phase in MG/L medium with 4 μg of tetracycline per ml and assayed. The values reported represent the average of three independent determinations.
[d] ND, Not determined.

vector pTJS75 (26). The resulting plasmid, pJW401, was then introduced into a *A. tumefaciens* A348, in which the VirB10Δ22-55-PhoA fusion protein had no alkaline phosphatase activity (Table 1).

Identification of VirB10 protein aggregates. Protein cross-linking reagents were used to further investigate the structure of VirB10 in the membrane. In these experiments, cells of strain A348 harboring pToK9 (14), a plasmid containing the *virG* gene from the supervirulent Ti plasmid pTiBo542, were used to increase the level of *virB10* gene expression. After AS induction, A348 pToK9 whole cells were treated with the membrane-impermeant protein cross-linking agent BS^3 (29). Because of its size (572 Da), BS^3 is capable of crossing through outer membrane pores into the periplasmic space but cannot penetrate the cytoplasmic membrane because of its hydrophilic nature. Treatment of whole cells with 200 μM BS^3 resulted in the appearance of three VirB10 protein aggregates with *M*a of 80, 115, and 140 kDa, respectively, in addition to the 48- and 39-kDa proteins (Fig. 7, lanes 1 and 2). Based on its immunostaining intensity, the 140-kDa molecule appeared to be the most abundant VirB10 aggregate. Identical results were obtained when A348 cells lacking pToK9 were subjected to cross-linking, but the levels of all the VirB10 protein products were reduced. The same VirB10 aggregates were also observed when purified inner membranes from AS-induced A348 pToK9 cells were treated with either 50 or 200 μM BS^3 (Fig. 7, lanes 4 and 5).

The subunit compositions of the VirB10 complexes were examined with the cleavable cross-linking agent DTBP (35). Preliminary experiments showed that concentrations of 2 to

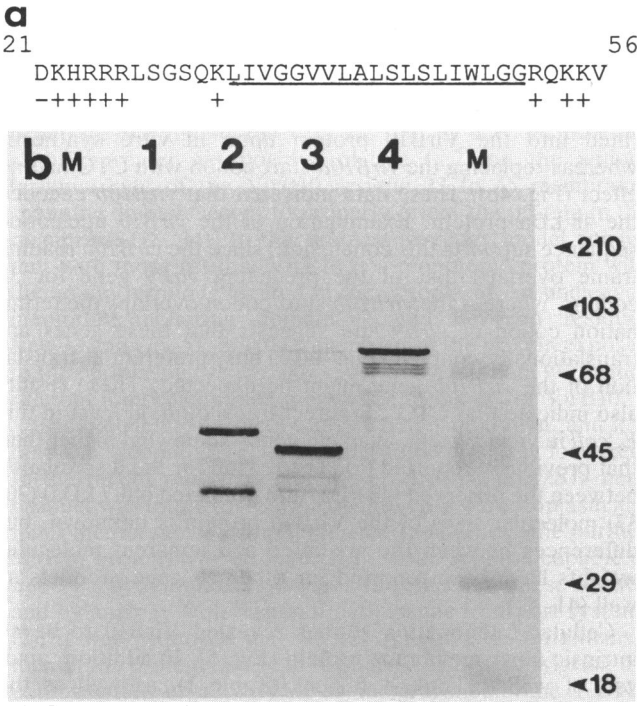

FIG. 6. (a) Predicted amino acid sequence of *virB10b* between residues 21 and 56 (37), showing a potential membrane-spanning region (underlined residues) identified by using the algorithms of Rao and Argos (24) and Klein et al. (16). The charged residues flanking the hydrophobic core are also indicated. (b) Identification of VirB10 and VirB10-PhoA fusion proteins containing a *virB10*Δ22-55 deletion. Cells of *E. coli* CC159 harboring various plasmids were grown in the presence of 1 mM IPTG for 2 h, and proteins were analyzed by SDS-PAGE and immunostaining with anti-VirB10 antiserum. Lane 1, pUC119; lane 2, pJW327; lane 3, pJW327Δ22-55; lane 4, p327-1Δ22-55; lanes M, molecular mass markers (in kilodaltons).

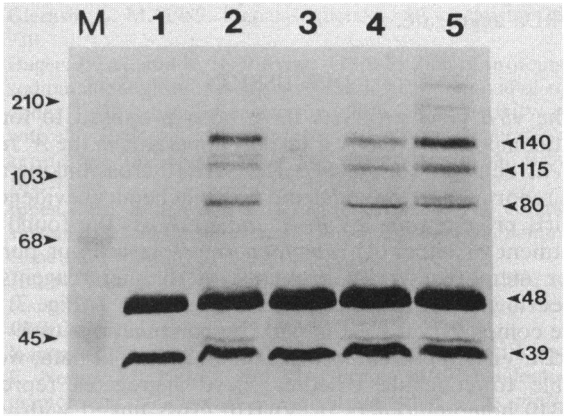

FIG. 7. BS^3 cross-linking analysis of the VirB10 protein. AS-induced *A. tumefaciens* whole cells or purified inner membranes were treated with BS^3 (29) and examined by one-dimensional SDS-PAGE (7% gel) as described in Materials and Methods. The proteins were then transferred to nitrocellulose and reacted with anti-VirB10 antiserum. Lane 1, Untreated whole cells; lane 2, whole cells treated with 200 μM BS^3; lane 3, untreated inner membrane; lane 4, inner membrane treated with 50 μM BS^3; lane 5, inner membrane treated with 200 μM BS^3; lane M, molecular mass markers (in kilodaltons). The positions and calculated molecular masses for the major cross-linked VirB10 complexes are indicated.

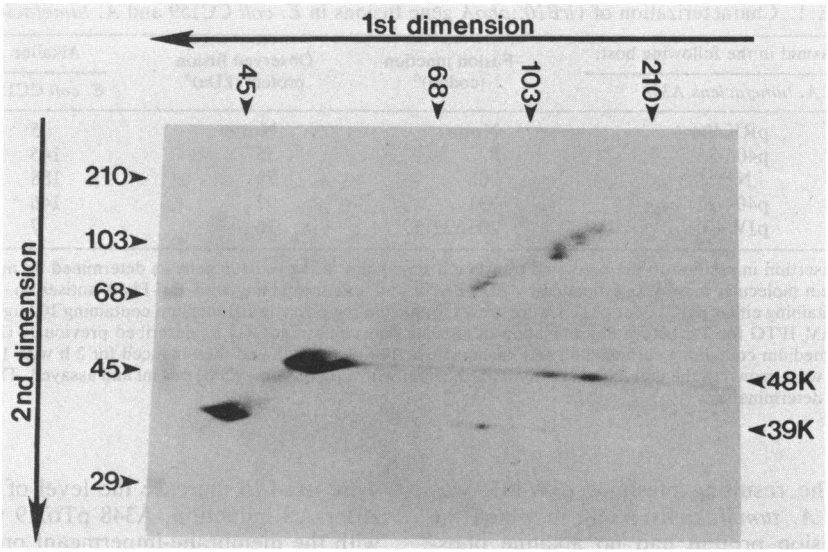

FIG. 8. Two-dimensional gel analysis of DTBP-cross-linked VirB10. Inner membrane proteins were cross-linked with 5 mM DTBP (35) and subjected to two-dimensional SDS-PAGE as described in Materials and Methods. The direction of migration during SDS-PAGE is indicated for each dimension. The positions of the VirB10 protein monomers and aggregates in the second dimension are indicated. Molecular masses are indicated in kilodaltons (K).

5 mM DTBP gave optimum results and generated the same VirB10 aggregates as BS^3. Inner membrane proteins were treated with 5 mM DTBP and then subjected to two-dimensional SDS-PAGE with reduction of the cross-links before electrophoresis in the second dimension. Upon reduction, the subunits of the cross-linked molecules migrated below the diagonal to positions dependent on their molecular weights. Immunoblotting analysis revealed that the *M*a 80-kDa aggregate yielded only the smaller 39-kDa VirB10 peptide as an off-diagonal component (Fig. 8). The reduced *M*a 115-kDa VirB10 aggregate appeared to contain the 48-kDa protein as a major component as well as a small amount of the 39-kDa protein. Finally, only the 48-kDa VirB10 protein was detected upon reduction of the *M*a 140-kDa aggregate.

DISCUSSION

The *virB* gene products have been proposed to form a multicomponent T-DNA transport apparatus in the *A. tumefaciens* cell wall (6, 36, 44). The VirB10 cross-linking analysis reported here provides the first biochemical evidence of a VirB protein complex in *A. tumefaciens*. We found that treatment of either *A. tumefaciens* whole cells or purified inner membranes with protein cross-linking reagents resulted in the formation of VirB10 aggregates (Fig. 7) that were composed, at least in part, by combinations of 39- and 48-kDa VirB10 protein forms (Fig. 8). From our data, we are unable to conclude whether these aggregates represent VirB10 homomultimers or VirB10 cross-linked with other proteins. The size and relative abundance of the 140-kDa aggregate we observed could be explained by the presence of a 48-kDa VirB10 protein trimer, with the smaller aggregates representing proteolytic breakdown products. However, further biochemical analysis will be necessary to determine the exact composition of these VirB10 complexes. The significance of the 39-kDa VirB10 peptide identified by immunostaining in both *E. coli* and *A. tumefaciens* is unclear (Fig. 3b). The 48-kDa protein appears to be the major *virB10* gene product, and it was the only VirB10 protein synthesized in vitro (Fig. 2, lanes 4 and 6). Thus, the 39-kDa protein might simply represent an in vivo breakdown product.

Two possible translation start sites located in tandem, designated *virB10a* and *virB10b*, are predicted by the *virB10* nucleotide sequence (30, 37) (Fig. 4a). We found that changing the *virB10b* start codon to CTG resulted in a nearly fivefold decrease in the amount of [^{35}S]methionine incorporated into the VirB10 protein upon in vitro synthesis, whereas replacing the *virB10a* start codon with CTG had no effect (Fig. 4b). These data indicated that *virB10b* encoded the 48-kDa protein. Examination of the *virB10* nucleotide sequence supports this conclusion, since the *virB10a* reading frame overlaps that of the preceding *virB9* gene for 32 codons, whereas the *virB10b* start codon overlaps the termination codon of *virB9* and suggests that these genes are translationally coupled (Fig. 4a). Thus, preferential translation of the *virB10b* gene might be expected. These results also indicate that CTG can direct translation, at least in this *E. coli* in vitro system, at an efficiency somewhat higher than that previously reported (5). The reason for the discrepancy between the observed (48 kDa) and predicted (40.7 kDa) (30, 37) molecular sizes of the VirB10 protein is unknown, but differences between the predicted and apparent molecular weights have been reported for other *vir* gene products as well (41, 42).

Cellular fractionation studies revealed VirB10 to be an intrinsic inner membrane protein (Fig. 5). In addition, analysis of *virB10*::Tn*phoA* fusions (Table 1), as well as the accessibility of VirB10 to the inner membrane-impermeant cross-linking reagent BS^3 in whole cells of *A. tumefaciens* (Fig. 7), indicated that VirB10 contained a periplasmic domain. We found that in-frame deletion of a potential membrane-spanning region between residues 22 and 55 (Fig. 6a) blocked translocation of a VirB10Δ22-55-PhoA fusion protein to the periplasm in both *E. coli* and *A. tumefaciens* (Table 1) and also prevented membrane insertion of the VirB10Δ22-55 protein in *A. tumefaciens* (data not presented). It is possible that structural changes caused by the deletion blocked membrane insertion in an indirect manner,

perhaps due to incorrect protein folding or impaired interaction with secretory factors. However, the predicted transmembrane structure and the location of the 327-25 *virB10*::*phoA* insertion immediately downstream (Table 1) both suggest a membrane-spanning role for this domain. Proteolytic processing of this region is unlikely, since a potential signal sequence processing site is lacking according to the "(−3, −1)-rule" of Von Heijne (32). In addition, we have found that the mobility in SDS-PAGE of the VirB10 protein synthesized either in vitro or in vivo is identical (data not presented), further suggesting that signal processing does not occur. We note that residues 22 to 55 represent an atypical topogenic element, as the 19-amino-acid hydrophobic core is flanked on the amino end by a net +5 positively charged region and on the carboxyl end by a net +3 positively charged region (Fig. 6a). This concentration of positively charged residues on either side of a membrane-spanning region is very unusual among bacterial exported proteins, probably because the basic residues do not easily penetrate the membrane (11, 23, 33). It may be that the slightly greater net positive charge (+2) on the amino-terminal side of the VirB10 residue 22 to 55 membrane-spanning domain serves to properly orient the protein in the membrane (18, 34). In the simplest topology model consistent with these results, VirB10 is a monotopic protein with the amino terminus located in the cytoplasm, an uncleaved membrane-anchoring domain located between residues Leu-33 and Gly-51, and the remainder of the protein exposed to the periplasmic space. However, from our data we cannot rule out a more complex membrane topology for VirB10.

The biochemical function of VirB10 is unknown, and it is only the second *virB* gene product to be precisely localized. In the recent report by Christie et al. (6), the *virB11* gene product was found to fractionate into both the cytoplasm and inner membrane of *A. tumefaciens*. In addition, the purified VirB11 protein was discovered to be an ATPase capable of undergoing autophosphorylation (6). Based on these results, and by analogy with bacterial periplasmic transport systems (2), it was proposed that VirB11 functions as an extrinsic membrane protein kinase to regulate via phosphorylation the conformation or activity of an integral membrane T-DNA transfer pore (6).

We have recently demonstrated that *virB10* is required for plant transformation (37a) and for the transfer to plant cells of a Mob^+ pRSF1010 derivative plasmid lacking a T-DNA border (J. Ward and A. Binns, unpublished data). Thus, the identification of a membrane-spanning VirB10 protein aggregate raises the possibility that VirB10 is a structural component of the T-DNA transfer apparatus.

ACKNOWLEDGMENTS

We thank Stephen Lory for the gift of alkaline phosphatase antiserum and Randall Kerstetter, George Bolton, Manjusri Das, and Larry Gold for helpful discussions.

This work was supported in part by Public Health Service grant 5 ROI GM 32618-14 from the National Institutes of Health to E.W.N. and National Science Foundation grants PCM 83-52434 to A.N.B. and DCB-88-19197 to A.N.B. and J.E.W.

LITERATURE CITED

1. **Albano, M., R. Breitling, and D. A. Dubnau.** 1989. Nucleotide sequence and genetic organization of the *Bacillus subtilis comG* operon. J. Bacteriol. **171**:5386–5404.
2. **Ames, G. F.-L.** 1986. Bacterial periplasmic transport systems: structure, mechanism, and evolution. Annu. Rev. Biochem. **55**:397–425.
3. **Binns, A. N., and M. F. Thomashow.** 1988. Cell biology of *Agrobacterium* infection and transformation of plants. Annu. Rev. Microbiol. **42**:575–606.
4. **Buchanan-Wollaston, V., J. E. Passiatore, and F. Cannon.** 1987. The *mob* and *oriT* mobilization functions of a bacterial plasmid promote its transfer to plants. Nature (London) **328**:172–175.
5. **Childs, J., K. Villanueba, D. Barrick, T. D. Schneider, G. D. Stormo, L. Gold, M. Leitner, and M. Caruthers.** 1985. Ribosome binding site sequences and function. UCLA Symp. Mol. Cell. Biol. **30**:341–350.
6. **Christie, P. J., J. E. Ward, Jr., M. P. Gordon, and E. W. Nester.** 1989. A gene required for transfer of T-DNA to plants encodes an ATPase with autophosphorylating activity. Proc. Natl. Acad. Sci. USA **86**:9677–9681.
7. **Christie, P. J., J. E. Ward, S. C. Winans, and E. W. Nester.** 1988. The *Agrobacterium tumefaciens virE2* gene product is a single-stranded DNA-binding protein that associates with T-DNA. J. Bacteriol. **170**:2659–2667.
8. **Ditta, G., T. Schmidhauser, E. Jakobson, P. Lu, X. Liang, D. R. Finlay, D. Guiney, and D. R. Helinski.** 1985. Plasmids related to the broad host range vector, pRK290, useful for gene cloning and for monitoring gene expression. Plasmid **13**:149–153.
9. **Engstrom, P., P. Zambryski, M. Van Montagu, and S. E. Stachel.** 1987. Characterization of *Agrobacterium tumefaciens* virulence proteins induced by the plant factor acetosyringone. J. Mol. Biol. **152**:183–208.
10. **Garfinkel, D. J., R. B. Simpson, L. W. Ream, F. F. White, M. P. Gordon, and E. W. Nester.** 1981. Genetic analysis of crown gall: fine structure map of the T-DNA by site-directed mutagenesis. Cell **27**:143–153.
11. **Gierash, L. M.** 1989. Signal sequences. Biochemistry **28**:923–930.
12. **Hager, D. A., and R. R. Burgess.** 1980. Elution of proteins from sodium dodecyl sulfate-polyacrylamide gels, removal of sodium dodecyl sulfate, and renaturation of enzymatic activity; results with sigma subunit of *Escherichia coli* RNA polymerase, wheat germ DNA topoisomerase, and other enzymes. Anal. Biochem. **109**:76–86.
13. **Ippen-Ihler, K. A., and E. G. Minkley.** 1986. The conjugation system of F, the fertility factor of *Escherichia coli*. Annu. Rev. Genet. **20**:593–624.
14. **Jin, S., T. Komari, M. Gordon, and E. W. Nester.** 1987. Genes responsible for the supervirulence phenotype of *Agrobacterium tumefaciens*. J. Bacteriol. **169**:4417–4425.
15. **Kanemoto, T., A. Powell, D. Akiyoshi, E. Regier, R. Kerstetter, E. Nester, M. Hawes, and M. Gordon.** 1989. Nucleotide sequence and analysis of the plant-inducible locus *pinF* from *Agrobacterium tumefaciens*. J. Bacteriol. **171**:2506–2512.
16. **Klein, P., M. Kanehisa, and C. DeLisi.** 1985. The detection and classification of membrane-spanning proteins. Biochim. Biophys. Acta **815**:468–476.

16a. **Kuldau, G. A., G. De Vos, J. Owen, G. McCaffrey, and P. Zambryski.** 1990. The *virB* operon of *Agrobacterium tumefaciens* pTiC58 encodes 11 open reading frames. Mol. Gen. Genet. **221**:256–266.

17. **Leroux, B., M. F. Yanofsky, S. C. Winans, J. E. Ward, S. F. Ziegler, and E. W. Nester.** 1987. Characterization of the *virA* locus of *Agrobacterium tumefaciens*: a transcriptional regulator and host range determinant. EMBO J. **6**:849–856.
18. **Li, P., J. Beckwith, and H. Inouye.** 1988. Alteration of the amino terminus of the mature sequence of a periplasmic protein can severely affect protein export in *Escherichia coli*. Proc. Natl. Acad. Sci. USA **85**:7685–7689.
19. **Maniatis, T., E. F. Fritsch, and J. Sambrook.** 1982. Molecular cloning: a laboratory manual. Cold Spring Harbor Laboratory, Cold Spring Harbor, N.Y.
20. **Manoil, C., and J. Beckwith.** 1985. Tn*phoA*: a transposon probe for protein export signals. Proc. Natl. Acad. Sci. USA **82**:8129–8133.
21. **Manoil, C., and J. Beckwith.** 1986. A genetic approach to analyzing membrane protein topology. Science **233**:1403–1408.
22. **Manoil, C., J. J. Mekalanos, and J. Beckwith.** 1990. Alkaline phosphatase fusions: sensors of subcellular location. J. Bacteriol. **172**:515–518.

23. **Oliver, D.** 1985. Protein secretion in *E. coli*. Annu. Rev. Microbiol. **39**:615–648.
24. **Rao, J. K. M., and P. Argos.** 1986. A conformational preference parameter to predict helices in integral membrane proteins. Biochim. Biophys. Acta **869**:197–214.
25. **Sartorelli, A. C., D. S. Fischer, and W. G. Downs.** 1966. Use of sarcoma 180/TG to prepare hyperimmune ascitic fluid in the mouse. J. Immunol. **96**:676–682.
26. **Schmidhauser, T. J., and D. R. Helinski.** 1985. Regions of broad-host-range plasmid RK2 involved in replication and stable maintenance in nine species of gram-negative bacteria. J. Bacteriol. **164**:446–455.
27. **Stachel, S. E., and E. W. Nester.** 1986. The genetic and transcriptional organization of the *vir* region of the A6 Ti plasmid of *Agrobacterium*. EMBO J. **5**:1445–1454.
28. **Stachel, S. E., and P. Zambryski.** 1986. *Agrobacterium tumefaciens* and the susceptible plant cell: a novel adaptation of extracellular recognition and DNA conjugation. Cell **47**:155–157.
29. **Staros, J. V.** 1982. *N*-Hydroxysulfosuccinimide active esters: bis(*N*-hydroxysulfosuccinimide) esters of two dicarboxylic acids are hydrophilic, membrane-impermeant, protein cross-linkers. Biochemistry **21**:3950–3955.
30. **Thompson, D. V., L. S. Melchers, K. B. Idler, R. A. Schilperoort, and P. J. J. Hooykaas.** 1988. Analysis of the complete nucleotide sequence of the *Agrobacterium tumefaciens virB* operon. Nucleic Acids Res. **16**:4621–4636.
31. **Vieira, J., and J. Messing.** 1987. Production of single-stranded plasmid DNA. Methods Enzymol. **153**:3–11.
32. **von Heijne, G.** 1986. A new method for predicting signal sequence cleavage sites. Nucleic Acids Res. **11**:4683–4690.
33. **von Heijne, G., and Y. Gavel.** 1988. Topogenic signals in integral membrane proteins. Eur. J. Biochem. **174**:671–678.
34. **von Heijne, G., W. Wickner, and R. E. Dalbey.** 1988. The cytoplasmic domain of *Escherichia coli* leader peptidase is a "translocation poison" sequence. Proc. Natl. Acad. Sci. USA **85**:3363–3366.
35. **Wang, K., and F. M. Richards.** 1974. An approach to nearest neighbor analysis of membrane proteins; application to the human erythrocyte membrane of a method employing cleavable cross-linkages. J. Biol. Chem. **249**:8005–8018.
36. **Ward, J. E., D. Akiyoshi, D. Regier, A. Datta, M. P. Gordon, and E. W. Nester.** 1988. Characterization of the *virB* operon from an *Agrobacterium tumefaciens* Ti plasmid. J. Biol. Chem. **263**:5804–5814.
37. **Ward, J. E., D. Akiyoshi, D. Regier, A. Datta, M. P. Gordon, and E. W. Nester.** 1990. Characterization of the *virB* operon from an *Agrobacterium tumefaciens* Ti plasmid. J. Biol. Chem. **265**:4768.
37a. **Ward, J. E., Jr., E. M. Dale, P. J. Christie, E. W. Nester, and A. N. Binns.** 1990. Complementation analysis of *Agrobacterium tumefaciens* Ti plasmid *virB* genes by use of a *vir* promoter expression vector: *virB9*, *virB10*, and *virB11* are essential virulence genes. J. Bacteriol. **172**:5187–5199.
38. **Willets, N., and R. Skurray.** 1987. Structure and function of the F factor and mechanism of conjugation, p. 1110–1133. *In* F. C. Neidhardt, J. L. Ingraham, K. B. Low, B. Magasanik, M. Schaechter, and H. E. Umbarger (ed.), *Escherichia coli* and *Salmonella typhimurium*: cellular and molecular biology, vol. 2. American Society for Microbiology, Washington, D.C.
39. **Winans, S. C., R. A. Kerstetter, J. E. Ward, and E. W. Nester.** 1989. A protein required for transcriptional regulation of *Agrobacterium* virulence genes spans the cytoplasmic membrane. J. Bacteriol. **171**:1616–1622.
40. **Yanisch-Perron, C., J. Vieria, and J. Messing.** 1985. Improved M13 phage cloning vectors and host strains: nucleotide sequences of M13mp18 and pUC19 vectors. Gene **33**:103–119.
41. **Yanofsky, M. F., and E. W. Nester.** 1986. Molecular characterization of a host-range-determining locus from *Agrobacterium tumefaciens*. J. Bacteriol. **168**:244–250.
42. **Yanofsky, M. F., S. G. Porter, C. Young, L. M. Albright, M. P. Gordon, and E. W. Nester.** 1986. The *virD* operon of *Agrobacterium tumefaciens* encodes a site-specific endonuclease. Cell **47**:471–477.
43. **Zambryski, P.** 1988. Basic processes underlying *Agrobacterium*-mediated DNA transfer to plants. Annu. Rev. Genet. **22**:1–30.
44. **Zambryski, P.** 1989. *Agrobacterium*-plant cell DNA transfer, p. 309–333. *In* D. E. Berg and M. M. Howe (ed.), Mobile DNA. American Society for Microbiology, Washington, D.C.
45. **Zambryski, P., J. Tempe, and J. Schell.** 1989. Transfer and function of T-DNA genes from *Agrobacterium* Ti and Ri plasmids in plants. Cell **56**:193–201.